

Characterizing Massive Star Feedback: From Hierarchical Collapse to Gas Expulsion

SEAN C. LEWIS¹

¹*Drexel University Department of Physics
Philadelphia, Pennsylvania*

(Received June 08, 2020)

Submitted to Drexel University Department of Physics

ABSTRACT

By using the software suite Torch, coupling stellar N-body dynamics, stellar feedback, and magnetohydrodynamics, I create numerical models of the star cluster formation process and characterize the behavior and effects of massive O-type stars via sets of controlled experiments. The star formation process begins with the gravitational collapse of giant molecular clouds to then form stars and ends with the clearing away of surrounding gas by way of massive star feedback. My research, following star formation from start to finish, will represent one of the most detailed numerical models of the process to date.

My continued work at Drexel will prepare me for the participation in post-doc positions continuing research on star formation and ultimately setting my path to become a professor at an undergraduate-focused university.

1. INTRODUCTION

Star formation is a very active area of research involving topics ranging from the dynamics of turbulent giant molecular clouds (GMCs), to the fusion processes within the stars themselves, to the galactic scale effects of star births. Although on vastly different length and time scales, all of these processes are interconnected and have their own set of active unanswered questions. My research focuses on the global hierarchical collapse of GMCs into filaments and stellar cores, the formation of individual stars and the interactions between stars and gas both gravitationally and energetically through stellar feedback, and the eventual ejection of gas from a star cluster via said feedback. A simplified star forming region (as seen in Figure 1) begins as a self-gravitating, cold (10 K), neutral, turbulent GMC several to tens of parsecs wide surrounded by warmer neutral hydrogen gas at 1e4 K. This cold and warm neutral media (CNM; WNM) are in pressure equilibrium, but regions of the turbulent cloud will become gravitationally unstable and collapse inwards, fragmenting and continuing to collapse until hydrogen fusion results in the birth of stars deeply embedded in gas. The most massive of the stars inject energy and matter back into the surrounding gas in the form of photoionizing photons and stellar winds. After a few Megayears, as more stars form, the system is considered an embedded cluster and after 10 or more Myr the gas is entirely removed from the system (see [Krumholz et al. \(2014\)](#) for an extensive overview of stellar feedback).

Since the star formation process takes place over several million years and in regions of very dense opaque gas, it is difficult for observational techniques to describe how star clusters become unembedded. The common assertion is gas is expelled from the star forming region via massive star feedback in the forms of ionizing radiation, stellar winds, and supernovae. To add to the complication, [Lada & Lada \(2003\)](#) find that 90% of all local embedded star clusters are destroyed before they become gas-free. This implies that star clusters must have been disrupted *prior* to the most destructive feedback mechanism, supernovae. The importance of photoionization and stellar winds is also an active area of research ([Dale, J. et al. 2012a, 2014](#)) but the most recent consensus is that *all* stellar feedback mechanisms play an important role in regulating the formation of stars in an embedded system and in the halting of star formation and ejection of gas. Photoionizing radiation from massive stars can create parsec scale regions of ionized hydrogen (known as HII regions). The resulting warm ionized medium (WIM) has a gas sound speed nearly 2 orders of magnitude greater than the surrounding CNM, greatly increasing the length scale on which continuous gravitational collapse will occur, effectively halting further fragmentation into dense stellar cores in the region. Stellar winds are likely a

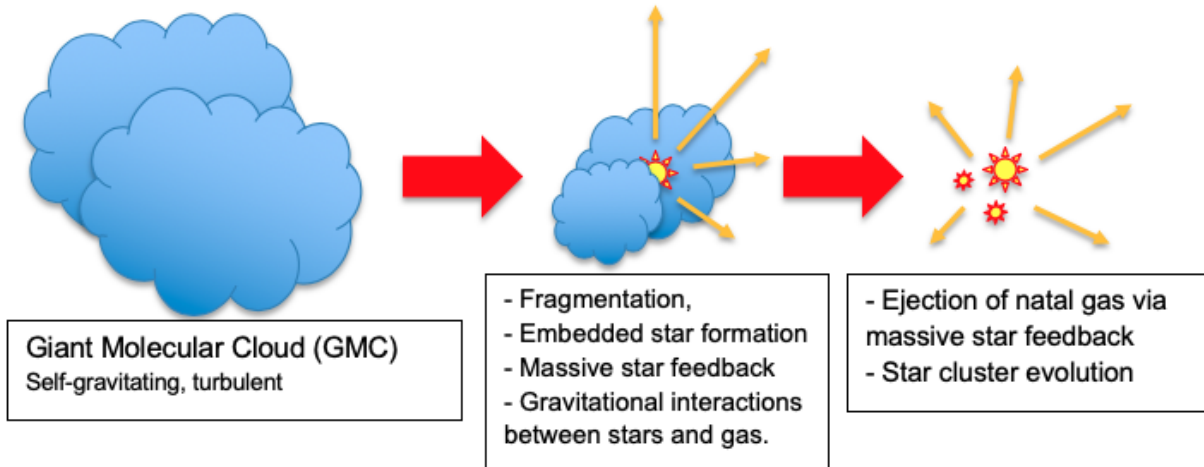


Figure 1. *The Star Formation Process.* Hierarchical collapse eventually results in gas fragmenting into filaments and stellar cores. If the cores contain massive stars, stellar feedback may begin disrupting the surrounding gas. If the disruption effects are great enough, star formation will eventually stop as gas is removed from the region. The entire process, beginning with the onset of collapse, can complete in less than 10 Myr.

more destructive force, the star's FUV emission rips material from the stellar atmosphere and deposits it into the surrounding medium at hypersonic velocities. O-type stars can inject $1e-6 - 1e-8 M_{\odot}/\text{yr}$ at velocities 2000 - 3000 km/s (Draine, B. 2011a). The hypersonic material shocks the surrounding gas to the order of $1e7$ K and carving a low density free-flowing wind cavity around the star. Finally, supernovae are by far the most abrupt destructive force, violently injecting momentum and energy into the surrounding media, disrupting regions tens of parsecs wide. Ionizing flux and stellar wind strength both scale strongly with star mass and are present and vary in intensity throughout a massive star's lifetime. Supernovae on the other hand are more consistent in their destructive force and are singular events at the end of a massive star's life and so only take effect after >3 Myr (Rahner, D. et al. 2017).

The extent to which massive star feedback is important in removing surrounding gas and significantly disrupting the stellar cluster during their normal lifecycle is not yet well understood. As stated before, lacking detailed observational data of the initial star formation and embedded dynamics necessitates the use of numerical methods (although infrared observatories such as ALMA are providing unprecedented glimpses into star forming regions, numerical methods are still needed to follow the collapse, formation, unembedding process from start to finish). However, star formation is a complex, multi-physics process taking place over millions of years and extending across spatial scales of several parsecs down to fractions of an AU. As such, simplifications must be made when designing simulations. In Dale, J. et al. (2012a, 2014) they use a smoothed particle hydrodynamics (SPH) code to model the collapse of a GMC. While they first only include photoionizing feedback stellar winds are later added. However, while modeling the two early feedback mechanisms, the Dale et al. series of studies are unable to resolve individual stars due to the limitations of SPH models. Instead, a single sink particle represents an entire star cluster except for the smallest star-forming clouds. They are therefore unable to analyze any self-consistent interactions between gas and individual stars and stars with themselves in a cluster environment. Similarly, Rahner, D. et al. (2017) model a 1 dimensional semi-analytic feedback model that does not follow the global hierarchical collapse of the GMC and instead investigates an already-formed star cluster also represented as a single object. Domínguez, R. et al. (2017) follows the evolution of individual star particles in a cluster structure but does not model include hydrodynamical behavior of the gas, instead they overlay a radially dependent potential and so are unable to self-consistently model stellar feedback effects on any surrounding gas. Gonzales (2020) does form individual stars from gas, but are unable to resolve the formation of stars of mass less than $0.3 M_{\odot}$, thereby neglecting a significant fraction of the dynamical components of a cluster. More robustly, Kroupa, P. (2001) include a time-dependent gas potential, simulating the expulsion of surrounding gas but still without explicitly modeling any stellar feedback. To most accurately model the entire star formation process from collapse to gas expulsion, individual stars must be resolved as well as their feedback in the presence of a coevolving, self-gravitating gas.

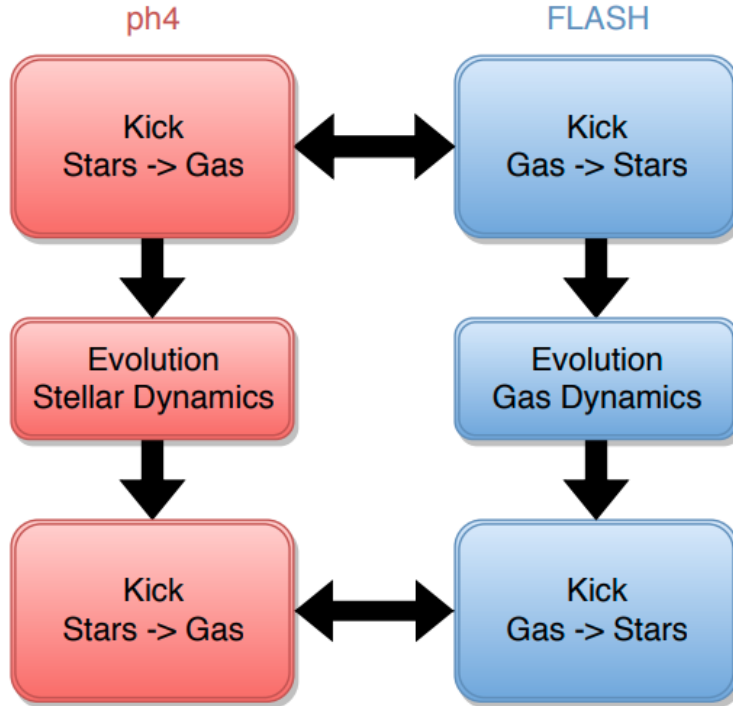


Figure 2. From Wall et al. (2019). The gravity bridge allows for the co-evolution of gas and star particles while communicating the gravitational effects within and between the two while also treating the evolution of individual stars.

Ultimately, a coupled N-body, stellar feedback, hydrodynamics model must be used to effectively determine the role which massive star feedback plays a role in the early disruption of embedded clusters and later gas expulsion, in addition to identifying any common morphological features due to massive star feedback.

2. NUMERICAL METHODS: TORCH

2.1. Overview

Torch (Wall et al. 2019) is a novel simulation technique that bridges gas dynamics with collisional N-body dynamics and individual stellar feedback. It accomplishes this by pairing the magnetohydrodynamics Eulerian grid code FLASH (Fryxell et al. 2000) and the N-body stellar evolution code AMUSE (Zwart & McMillan 2018). Torch combines the physics of gas heating through a wide range of densities, magnetic fields, dynamical effects between individual stars and their natal gas cloud, formation of binaries and higher order systems, and stellar feedback in the form of radiation, winds, and supernovae for stars $>7 M_{\odot}$. To gravitationally couple the N-body and gas, Torch evolves the stars and gas in parallel, communicating gravitational "kicks" (Figure 2).

Individual stellar evolution is handled by SeBa (Portegies Zwart & Verbunt 1996). For massive stars, the particle's age, initial mass, and simulation time step are used to determine the star's ionizing radiation flux and the mass and velocities of ejected winds. This information is passed to FLASH which then injects the winds into surrounding cells and uses a modified raytracing algorithm FERVENT (Baczynski, C. et al. 2015) to trace ionizing rays from the massive star.

FLASH acts as the container of the simulation space, defining the physical region where physics are implemented. FLASH is a Eulerian grid-based magnetohydrodynamics (MHD) code with adaptive mesh refinement (Olson & MacNeice 2005). In regions where gas density exceeds the Jeans criterion, AMR allows for the simulation grid (MacNeice et al. 2000) to be subdivided into smaller cells (representative of more compact spacial regions and therefore more detailed gas structure). This allows for higher resolution and detail in regions where gravitational collapse of the gas is progressing while leaving gravitationally stable gas at lower resolution thereby reducing total computation time while tracking the hierarchical collapse of the gas.

The gas handled by FLASH is heated by a background energy deposition of galactic FUV flux and cosmic rays. The dust cools via atomic and dust cooling. As a result, the gas has three distinct phases that can exist in pressure equilibrium, specifically the cool and warm neutral mediums (CNM, WNM) and very hot shocked gas (McKee & Ostriker 1977). Of note is the agreement of Torch’s CNM and WNM pressure equilibrium to Wolfire et al. (2003).

Additionally, Torch treats star particles in FLASH, ph4 (McMillan et al. 2012), and SeBa as a single data structure. Such a unique combination is extraordinarily powerful and allows for the exploration of many topics within the star formation process. Torch provides a set of tools to self-consistently model and analyze the star formation process in its entirety, and importantly allows for the analysis of the transition from an embedded star cluster to a cluster devoid of gas.

Torch’s adaptive mesh refinement (AMR) computational space allows for high levels of resolution in regions of interest. In the case of star formation, such regions are those of Jean’s unstable gas (Jeans, J. H. 1902) collapsing to form stars which can extend a few hundredths of a parsec, about one thousand times smaller than the scale of the full simulation space. Therefore, the star forming regions constitute a large number of computational grid cells. Each grid cell interacts gravitationally with surrounding cells, are heated by background radiation, and employ a hydrodynamical Riemann solver for each grid face to determine gas flow. In addition, star-gas, gas-star, and star-star interactions must be calculated. Finally, the computational domain must be evolved thousands of times per simulation run. Each simulation is therefore be very computationally expensive and parallelization across HPC architecture is absolutely necessary. To efficiently process my simulation data, I use the Python data visualization package yt (Turk et al. 2011).

With Torch, I design a set of controlled experiments of a star forming region where I will alter the first star to form in a central region of a collapsing giant molecular cloud (GMC) to be an O-type star of 8, 20, and 50 M_{\odot} while keeping initial conditions and physics constant. The GMC is a 7 pc wide 10,000 M_{\odot} self-gravitating turbulent sphere with a gaussian density profile (Dale, J. et al. 2012a, 2014). Then, through analysis of cluster and gas structure and dynamics I will be able to examine if any resulting patterns are largely stochastic or generated by the O-star formation.

2.2. Creating Stars

The collapse of gas cannot be numerically followed indefinitely. Eventually the spatial scales necessary to resolve the gas behavior will result in prohibitively small time steps. Instead, given a user-defined highest level of refinement, sink particles (Federrath et al. 2010) are used to represent regions of gas whose density exceeds ρ_{thresh} , corresponding to the smallest resolvable Jeans length defined by the Truelove criterion (Truelove et al. 1997) $2.5\Delta x$, 2.5 times the smallest cell size.

$$\rho_{thresh} = \frac{\pi c_s^2}{G\lambda_J^2} = \frac{\pi c_s^2}{G(2 * 2.5\Delta x)^2} \quad (1)$$

Then a spherical test volume V with radius r_{acc} (again satisfying the Truelove criterion) is centered around the cell that exceeds ρ_{thresh} . Then, the following checks are made: If all checks are passed, mass is removed from all cells within V until each has a density equal to the density threshold. The sink particle is then placed at the central cell and all removed gas mass is assigned to the sink particle. In addition to the conservation of mass during the formation, the conservation of linear and angular momentum is also upheld: the momentum of the removed gas is summed and assigned to the sink.

At this point, the sink behaves as a Lagrangian particle: permitted to move around the simulation space (always being centered at a single cell) and can be acted upon by the gravity of surrounding gas.

Once created, the mass of the sink itself and the gas mass within the cells on which the sink sits results in infalling gas, increasing the gas density within the cells in and around the sink. If any gas density within the sink’s r_{acc} exceeds the density threshold, is infalling, and is bound to the sink, the sink will accrete the excess gas. Then, a randomized list of star masses derived from the Poisson sampling of the Kroupa initial mass function (IMF) (Kroupa, P. 2001) is assigned to the sink. This stellar mass list accompanies the sink for as long as it exists and can be altered by the user to force any star mass to form in any order they please. Once the sink accretes enough gas mass to be equal to the next star on the list, the corresponding mass is removed from the sink and an AMUSE star particle is placed within the sink.

2.3. Stellar Feedback: Radiation, Winds, Supernova

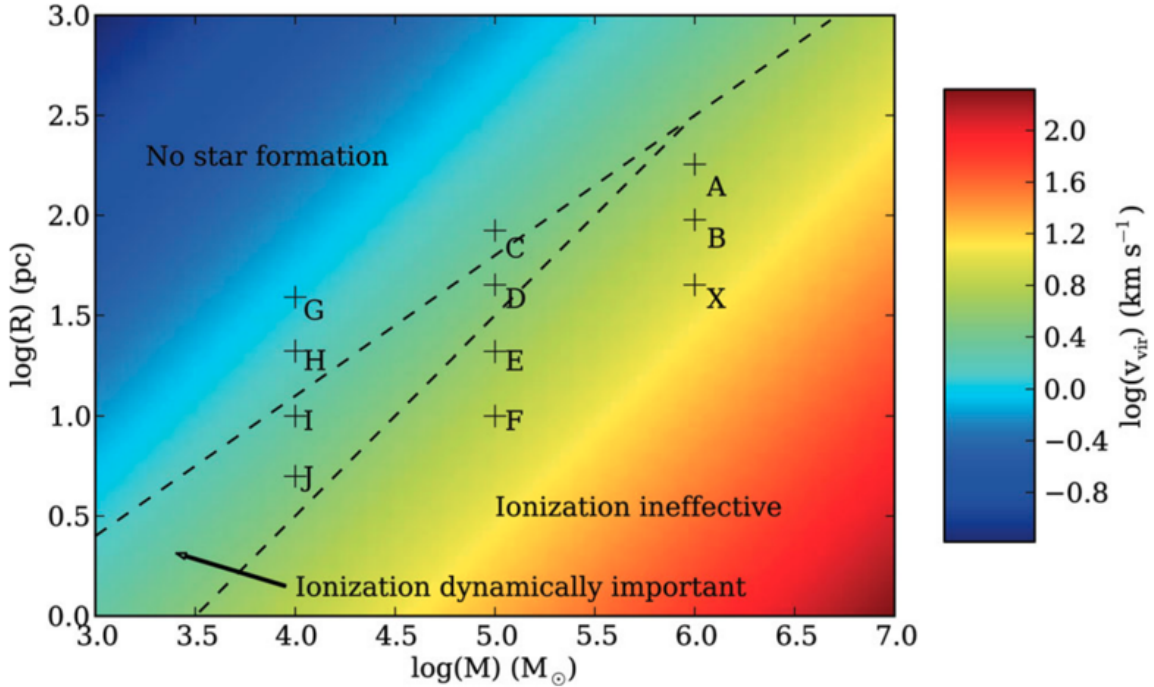


Figure 3. Results from Dale, J. et al. (2012a). Using SPH models, they determine the mass-radius parameter space of giant molecular clouds where ionizing radiation plays a critical role in regulating star formation. If the star-forming clouds are too diffuse (top-left) ionization is destructive enough to halt star formation entirely. If clouds are too dense (bottom-right), ionizing radiation is not able to penetrate far into the interstellar gas surrounding massive stars and so its effects are too localized to limit large-scale star formation.

Radiation from stars comes in two distinct energy bins. First is ionizing radiation ($E_\gamma > 13.6$ eV). The luminosity and average energy of ionizing photons are calculated via the stellar evolution temperature and mass by either interpolating the OSTAR2002 grid (Lanz & Hubeny 2003) if $T_\star > 27.5 \times 10^3$ K or estimated from the star’s blackbody curve (Stahler & Palla 2008) if $T_\star < 27.5 \times 10^3$ K. The ionizing radiation flux is then delivered to the grid cells via the built in FLASH ray tracing module FERVENT (Baczynski, C. et al. 2015) where the gas heating, momentum, and ionization fraction is then calculated.

The second energy bin is for the dust photoelectric effect (PE) from far UV (FUV) photons (5.6 eV $< E_\gamma < 13.6$ eV). PE photons are especially important for low mass stars ($7M_\odot < M_\star < 13M_\odot$), indeed Wall et al. (2019) find that unrealistic ultra-compact HII regions form in gas $n \gtrsim 10^6$ without the consideration of PE photons. In addition, PE photons have a much smaller cross section than ionizing photons and so are able to penetrate farther into the surrounding gas.

Dale, J. et al. (2012a) find that ionizing radiation is dynamically critical to regulating star formation in a subsection of GMC mass-radii combinations; . The simulations I detail in this proposal most closely correspond to clouds I and J in Figure 3, within the parameter space where the clouds are not too dense for ionization to be ineffective, and not too diffuse where ionization alone prevents all star formation.

Stellar winds are described previously, their implementation in Torch agrees with the theoretical model of Weaver et al. (1977); Figure 4 (Left). Winds are particularly destructive to the surrounding gaseous medium as the rapid and high-velocity deposition of matter into the region around a massive star produces confined, very hot ($T \sim 10^6 - 10^8$ K) bubbles. The bubble expands adiabatically and stellar wind is shocked as it encounters the bubble boundary expanding out into the cold, dense surrounding medium. After expanding, the wind bubble cools, and the free flowing winds continue to deposit momentum directly into the shell as ram pressure, thereby holding back the surrounding shocked wind region and ambient interstellar gas despite the bubble being rarified and under-pressured. Early on, the shocked wind will pile up a shell of shocked interstellar gas which becomes progressively smaller as the shock expands.

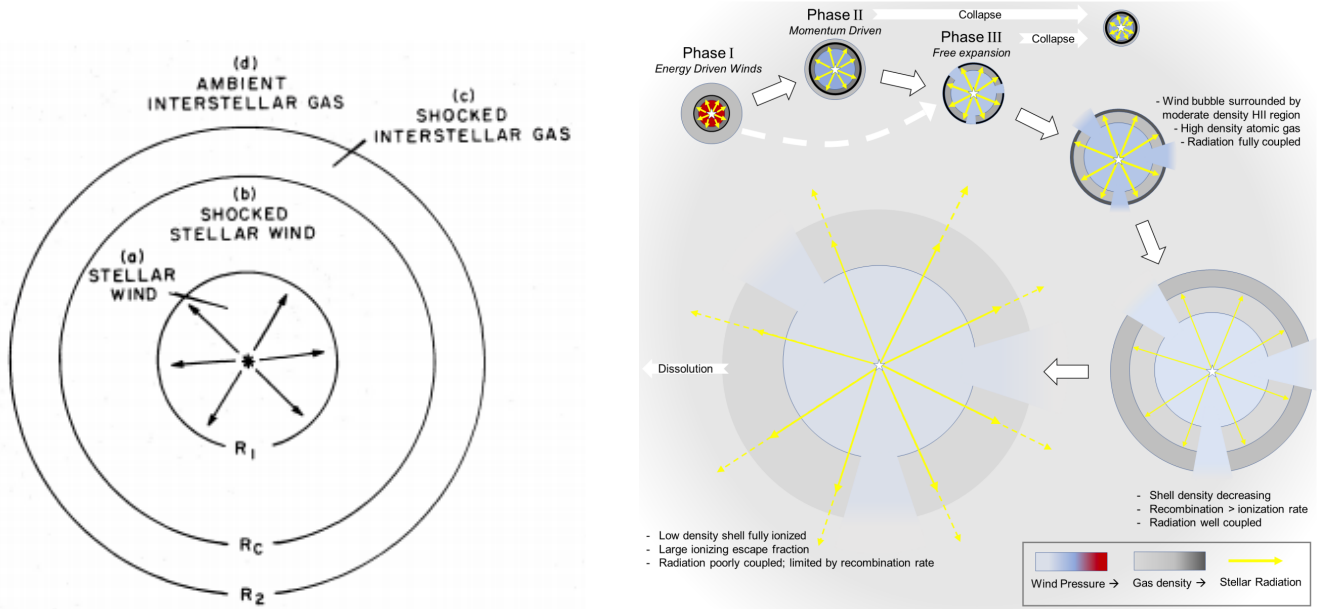


Figure 4. *Left:* Weaver et al. (1977) theoretical model. The wind bubble at this point has evolved to a free-flowing, rarified stream of matter (a) emanating from the central star that deposits momentum in the inner edge of R_1 , shocking the wind in the process (b). The shocked wind region will remain substantial in size and temperature and will remain so due to the long cooling time of shocked gas compared to the cool ambient interstellar medium. In low resolution simulations, $R_c \approx R_2$. *Right:* Rahner, D. et al. (2017) present a more detailed semi-analytic model that includes the fact that stellar winds and ionizing radiation work in conjunction to expand the wind bubble into a progressively more ionized region that eventually breaks down allowing radiation and free-flowing winds to escape the confinement of the ambient interstellar medium.

The injection of winds into the surrounding medium, generating a rarefied free-flowing wind bubble can result in the halting of star formation in the region. With Torch specifically, the rarefaction of gas will prevent any cell from exceeding the density threshold and so no further accretion into a sink particle can occur. With the lack of gas accretion, new star particles will be prevented from forming.

2.4. Ignored Subgrid Physics

As with any numerical model, there is a limit to how much can be simulated and ultimately some assumptions must be made. The mechanisms by which massive stars form are still a matter of debate. In the competitive accretion model, stars forming at the center of the local cluster gravitational potential grow more massive either by accretion of infalling gas or via merger events (Bonnell et al. 2004). In the turbulent core model, massive stars form in the same way low-mass stars do, except further fragmentation of their more massive stellar cores is halted by turbulent, radiative, and magnetic support (McKee & Tan 2003). In Torch, regions of gas at the highest refinement that is gravitationally unstable is removed from the grid and replaced with a sink particle. This means that any further fragmentation, behavior of the collapsing gas, or how and where massive stars form is assumed and not simulated.

It is widely understood that star clusters eventually become mass segregated (the migration of higher mass stars to gravitational potential minimum of the system) via the transfer of kinetic energy from the most massive cluster members to low-mass counterparts. In fact, there is recent observational evidence that mass segregation of clusters may occur *while* the cluster is forming when stellar cores are still accreting matter rather than after the formation process is completed (Plunkett et al. 2018).

This does give rise to some interesting choices, since Torch does provide control over how star particles are placed inside of star forming regions represented by the sink particle, we may choose to implement primordial mass segregation.

3. PAPER I: CHARACTERIZATION OF THE EARLY EFFECTS OF O-STAR FORMATION

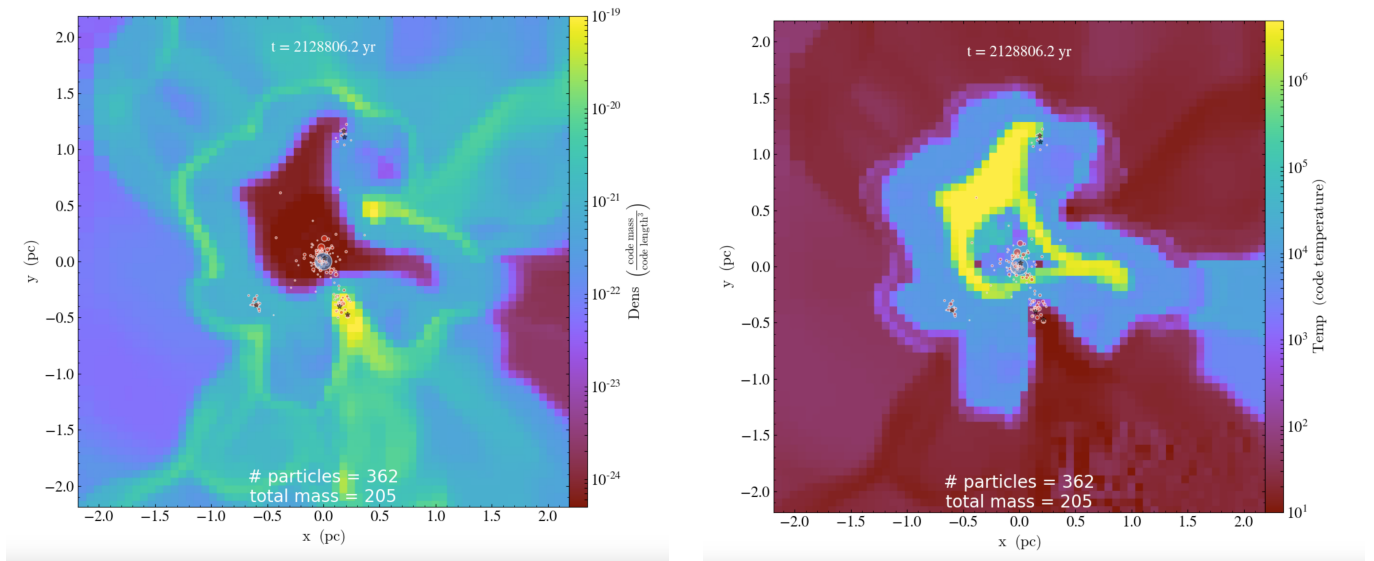


Figure 5. $50 M_{\odot}$ simulation. Left: Density (g/cm^3); Right: Temperature (K). Snapshot 123 kyr after $50 M_{\odot}$ star is placed onto the grid. The star generates a 2 pc wide ionized region and a free-flowing wind bubble 0.5 pc wide. Separating the two regions is the wind shocked gas at $>1\text{e}6$ K. Notice position $(+0.25, -0.5)$ pc a sink particle is confined to a dense column of gas which is not seen in the other runs. In addition, ionizing radiation leaks from the CNM into the surrounding MNW at $(+2.0, 0.0)$ pc.

We design a set of three Torch simulation with identical initial conditions modeling the global hierarchical collapse of a 7 pc wide spherical, turbulent GMC of $10,000 M_{\odot}$ with a gaussian density distribution (Dale, J. et al. 2012a, 2014). The spherical cloud comprised of molecular gas in the cold neutral medium (CNM) phase and is in pressure equilibrium with surrounding warm neutral medium (WNM). The pressure balance ensures the resulting collapse is due to turbulent behavior and self-gravitating effects. After 0.43 global free-fall times (1.32 Myr), a sink particle in the central dense region forms. I then edit the stellar mass list of the sink such that the three runs will begin forming an 8, 20, or $50 M_{\odot}$ star. Once the star forms, qualitative and quantitative analysis of the surrounding gas and subsequent star formation allows for the controlled characterization and identification of O-type star feedback effects. As expected, the $8 M_{\odot}$ star is unable to disrupt the gas it is born into. In the ideal case, the star’s Strömngren sphere, the region of cold gas it is able to photoionize, is a fraction of a single cell width.

$$r_S = \left(\frac{3S\mu^2 m_H^2}{4(1.1)\pi\alpha_B \rho_0^2} \right)^{1/3} = 2.8 S_{49}^{1/3} n_2^{-2/3} \text{pc} \quad (2)$$

The $50 M_{\odot}$ star inflicts the most destruction on the surrounding interstellar gas, even piercing through the enveloping CNM allowing for ionizing radiation to leak into the WNM background gas. The free-flowing wind bubble and shell of low-density high temperature shocked wind can each be seen clearly in Figure 5. The wind bubble cavity has dropped the local cell mass density several orders of magnitude lower than the density threshold set for sink particle creation, thereby preventing any more stars or other sinks to be spawned in the surrounding few pc^3 . At this low resolution, the distinction between shocked wind and shocked ISM material (R_c and R_2 in Figure 4) is not resolvable. Looking closer, star formation is occurring in a dense column of gas located at $(+0.25, -0.5)$ pc not seen the in the other massive star environments. This may be an instance of triggered star formation but further analysis is necessary to confirm such a claim. In addition, it is unclear at the moment if the rapid expulsion of gas from the gravitational potential of the sub-cluster in which the $50 M_{\odot}$ star is forming has caused any ballistic expansion of the stars either via the loss of the gas potential or gravitational influence of the expanding gas shell.

The $20 M_{\odot}$ star has less destructive influence. While the warm ionized HII region is still well resolved (see Figure 6 Right), the free-flowing wind bubble is not. There is still a very hot diffuse region 7 cells (~ 0.25 pc) wide that constitutes the shocked wind. This is expected as, the wind bubble is confined within the surrounding high pressure

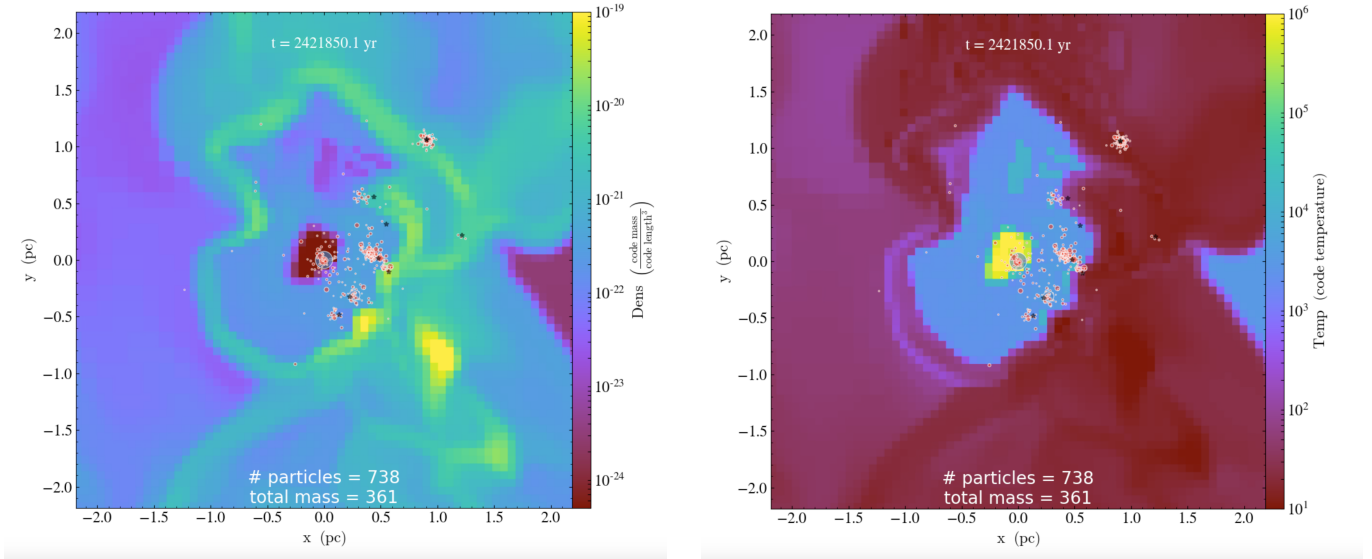


Figure 6. $20 M_{\odot}$ simulation. Left: Density (g/cm^3); Right: Temperature (K). Snapshot 582 kyr after $20 M_{\odot}$ star is placed onto the grid. The star generates a 1 pc wide ionized region. The wind shocked gas is well contained to a 0.25 pc (about 7 grid cells) wide region. No ionizing radiation has been able to escape the CNM. The $20 M_{\odot}$ star has been able to escape the potential well occupied by its parent sink. Therefore, star formation is completely halted in the subcluster containing the $20 M_{\odot}$ star and will not begin again unless another sink forms there or falls into the subcluster.

WIM generated by the ionizing emissions of the star and so the wind ram pressure will be on the order of the surrounding pressure at a distance of less than a cell size is expected to reach equilibrium with the ambient interstellar gas at a diameter less than a cell-width, unresolvable here. Although the shocked wind cavitation may still be enough to prevent gas accretion in the region, it is unclear if the wind structure will collapse as the star ages and its rate of mass loss diminishes.

The $8 M_{\odot}$ star is unable to inflict any significant disruption of the surrounding ambient stellar medium. This is also expected, as in equation (2) it can be shown that the $8 M_{\odot}$ star will create an HII region Strömgren sphere with a radius of a fraction of a single cell. So, even the ionization effects of the star are unresolvable. This behavior is confirmed in the phase plot (Figure 8) showing that no gas in the surrounding $10 pc^3$ has been heated either by ionization or wind shocks. There does exist a few solar masses of gas that exist at a high density, warm temperature state. This is likely the residual effects of the $8 M_{\odot}$ star heating its cell in which it sits and that energy diffusing to neighboring cells. Ultimately, this results in the continued accretion of gas onto the sink(s) contained within the main cluster structure at the center of Figure 7. Unless another massive star is allowed to form in the region, gas accretion will continue until all infalling matter is converted into star particles, a highly unrealistic scenario.

3.1. Comparison to similar work

Gonzales (2020) performs a similar study to quantify the effects of O-type star radiative feedback on surrounding molecular clouds and subsequent star formation. They claim to be able to test the global hierarchical collapse (GHC) scenario of molecular clouds (MC) and its ability to create realistic star clusters as well as pinpoint the precise effects of a single source of feedback on a cluster.

They cite the unrealistic nature of a perfectly spherical cloud collapsing and so explicitly model a collision between warm neutral medium (WNM) structures (two cylinders of same density and temperature as the background: $T=5000\text{K}$, $n=1\text{cm}^{-3}$ converging at 5.9km/s Mach 0.8) and the resulting compression and increase in density at the interface triggers a phase change to the cold neutral medium (CNM). A similar set of initial conditions is used in Dobbs et al. (2020).

Similarities to my methods. They use an AMR grid code (Colin, P. et al. 2013) that refines on density (similar to how Torch refines on Jeans length). They employ a method of self-consistent star placement, forming star particles straight from the grid. However, due to the minimum possible Jeans mass is set by the smallest refinement cell and

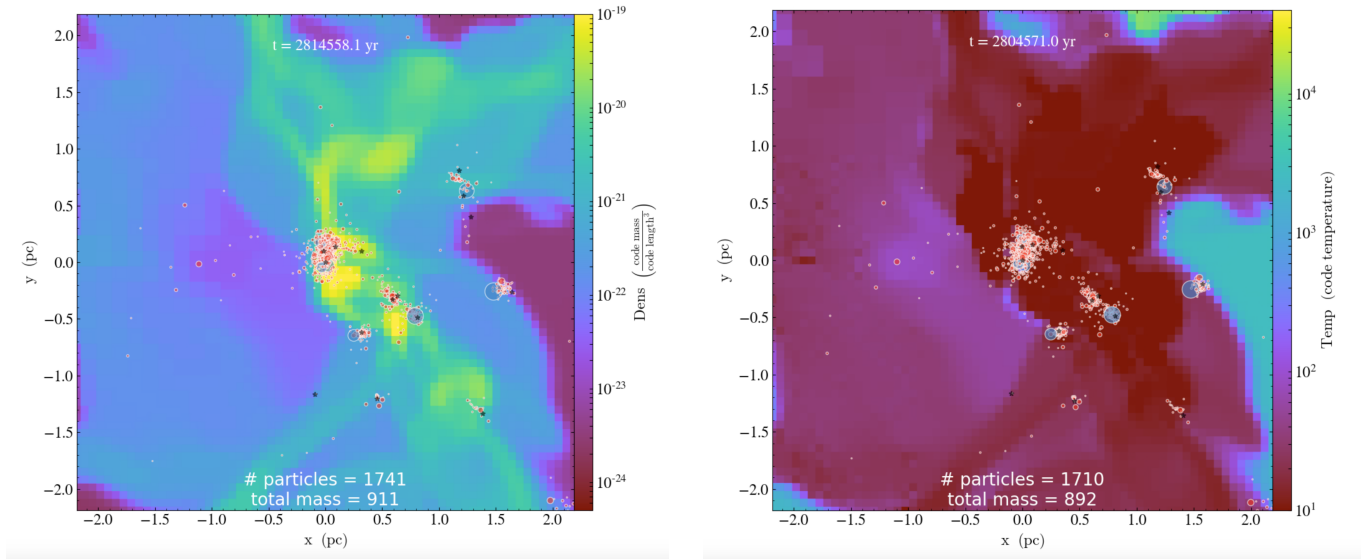


Figure 7. $8 M_{\odot}$ simulation. Left: Density (g/cm^3); Right: Temperature (K). Snapshot 1.12 Myr after $8 M_{\odot}$ star is placed onto the grid. The star is entirely unable to generate a visible ionized HII region. In addition, no wind shocked gas is visibly present.

so [Gonzales \(2020\)](#) are unable to form stars with masses less than $0.3M_{\odot}$. [Gonzales \(2020\)](#) also only include radiation feedback from massive stars, neglecting stellar winds and supernova.

4. TIMELINE: THE NEXT FEW YEARS AND BEYOND

4.1. 2019

In the last year, I have made significant progress towards my first publication as well as in my understanding and usage of Torch. In attempts to supplement my allotted computation time on Cartesius and funding from Drexel, I have applied to the Frontera Fellowship grant and an internship position at Los Alamos National Lab. Though both were declined, I will reapply this coming Fall. In addition, I have become increasingly involved in the upkeep and progression of Torch. Most recently, I successfully ported Torch’s FLASH to the latest released version (4.5 to 4.6.2; regression tests pending) and am confident in my ability to continue software updates of Torch components.

4.2. 2020

Priority one of the remaining half of the year is completion of my 3 runs in preparation for Paper 1. A run “completing” means pushing the simulation until the stars I have forced to form go supernova. The main obstacle is a matter of computation time. As of June 2020, FLASH4.5 is used in Torch. Commonly, FLASH will hang while passing around MPI buffers to fill grid guard cells after 9-12 hours of wall-clock run time. While this does not prevent runs from progressing (a simple restart from the last checkpoint output will continue past the stall point) it is preferred to be able to run simulations on Cartesius for the maximum time allotment of 120 wall-clock hours. Updating FLASH to the latest 4.6.2 version will potentially fix this issue (word of mouth suggests so) but at the very least allows myself to productively communicate with the FLASH development team rather than trying to debug an out of date version.

Once the 3 runs detailed in this proposal reach the first supernova detonation, the runs in their entirety can then be analyzed and reported in Paper I. Which I will complete and submit in late Fall of this year. I expect the analysis and writing process to take at least two months. I have allotted more time to provide room for inevitable revisions.

While the 8, 20, 50 M_{\odot} runs progress, I will design a simple recipe for testing different possible star particle initial position and velocity prescriptions. As discussed, this is an active conversation among Torch users and deserves investigation. This investigation would not constitute a paper in itself (although it could be twisted into a stand-alone technical paper) but instead be an appendix addition to Paper 2 (since any changes to the star particle placement methods would not be present in the Paper 1 runs).

4.3. 2021 - 2022

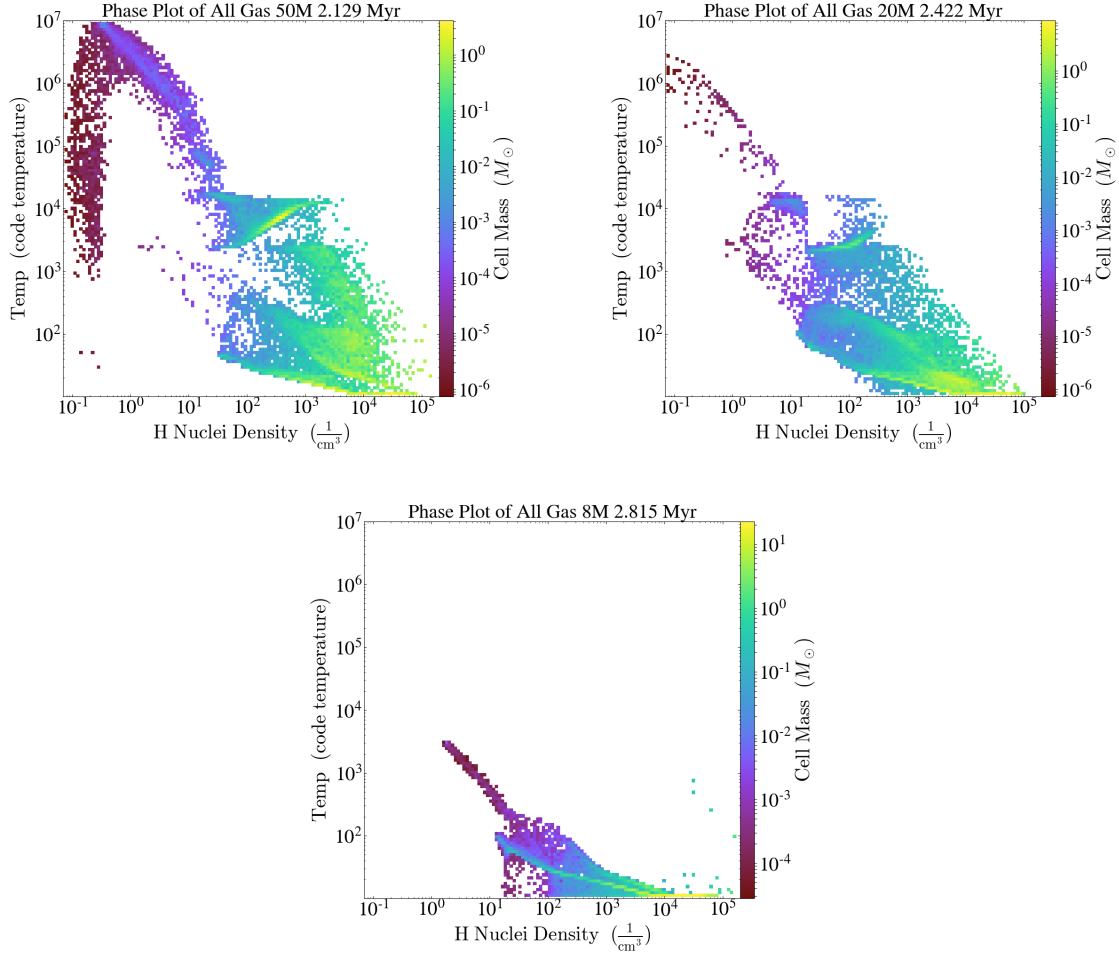


Figure 8. *Phase Plots of Runs.* Encompassing a 10^3 pc region around each massive star, details how much gas mass is in a state defined by Temperature (K) and Hydrogen number density (n^{-3}). Any gas that exists at temperatures in excess of $\sim 10^6$ K is shocked winds as the diffuse free-flowing wind bubble rams up against the surrounding denser ionized HII region. Ambient stellar media that has been ionized will lie in the $10^3 - 10^4$ K temperature range and, depending on its proximity to the outflowing wind shock, $10^1 - 10^3 \text{ cm}^{-3}$ number density. $50 M_{\odot}$ star (*Top Left*); $20 M_{\odot}$ star (*Top Right*); $8 M_{\odot}$ (*Bottom*)

After Paper I is submitted, I will begin expanding the parameter space of star masses forced to form to include 40, 75, and $100 M_{\odot}$ stars. In addition, these three new runs will be at a level of refinement higher than the Paper I runs and include the results of the previously mentioned star particle placement method improvements. The ambition is to submit Paper II my mid-year 2021, I anticipate the analysis to take less time as Paper I as analysis methods will have already been developed.

In early Winter quarter, I will also reapply to both the Frontera Fellowship and Los Alamos Graduate Research opportunities, both of which include travel to sites on location (of course the pandemic may force significant changes to this) and offer extensive interaction with HPC experts and other scientists.

After Paper II is submitted, I will begin to analyze the stellar dynamics of my half-dozen runs as unembedded clusters. By initializing the same star cluster in AMUSE only and evolving the system for a timescale on the order of Gigayears, we will be able to compare aged cluster dynamics and mass distributions with observations of clusters in the Milky Way. The computational requirements would be significantly less than the prior runs as FLASH MHD methods are not needed here. This work will constitute Paper III to be submitted in late Fall 2021.

4.4. 2022 - 2023

In my fifth year, I will again expand upon Papers I, and II. Here, I will embed my simulations in a larger galactic context. This may be something like including a background galactic potential to analyze the effects of gravitational

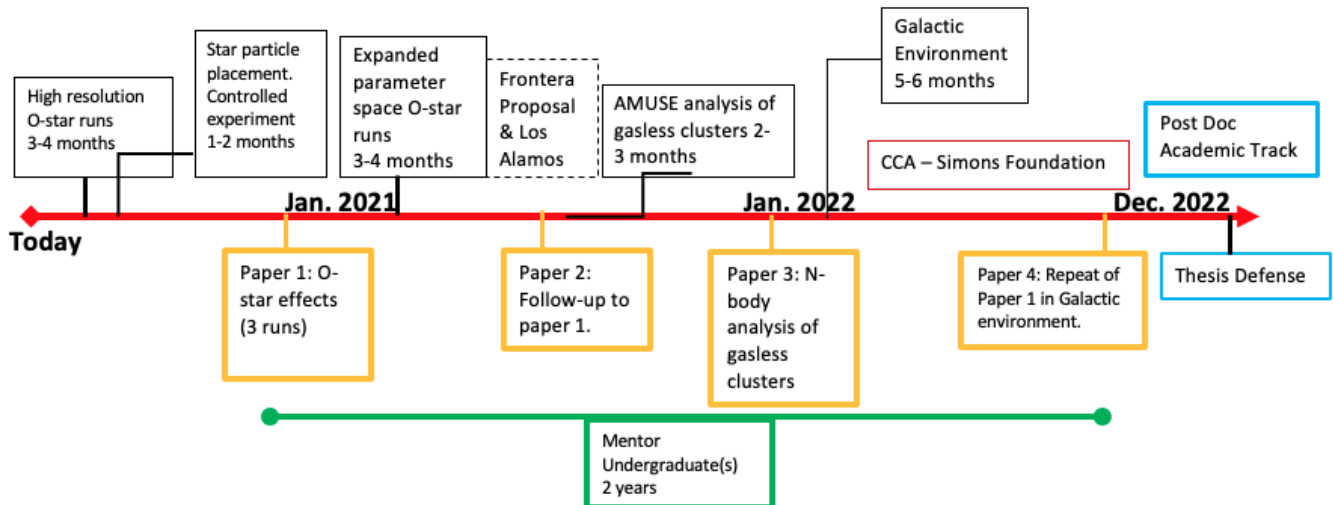


Figure 9. *Timeline.* The boxes in black are long-term items of work along with estimated completion times. The orange are the papers I will publish, other colors are for decoration. I will publish 4 papers, mentor one or more graduate students and continue to work in collaboration with national and international Torch users as well as continue the upkeep and development of Torch software and methods. In addition, I will reapply to the Frontera Fellowship and Los Alamos National Lab internship. I will also complete the PROFESS program at Drexel. Ultimately, my efforts will be to best prepare me for applications to post doctoral positions at Universities. The timeline begins "Today" (Summer 2020) and ends Winter 2022 constituting 2.5 years of work.

shear on the GMC and embedded star cluster. Or, by placing a star cluster that is about to have its first supernova into a galactic simulation, the larger scale effects can be monitored such as champagne flows. This would constitute Paper IV.

This effort may require significant collaboration amongst Torch users (collaborative efforts with Torch already exist and I address this in the final section), or outside experts. I hope to use the necessity for a larger-scale cooperative effort to establish a well-founded application to the Simons Foundation Center for Computation Astrophysics.

I will defend my thesis with the inclusion of four papers in late Fall 2022.

4.5. Aspirations

I see future me as a professor at a smaller college/university where the focus is on undergraduate research and learning. To achieve this goal, I need to prepare myself professionally for a post doctoral position at a university. It is my understanding that universities typically value their applicant's total number of publications. My timeline reflects this, I aim to produce a series of individual papers (some follow-ups of others) rather than compiling years of work into a single publication.

In addition, I will greatly improve my acceptance prospects for post doctoral positions by completing the PROFESS graduate course sequence offered at Drexel. PROFESS requires attendance and work associated with classes beginning in the Fall of 2020 and completing in the Summer 2021. Furthermore I will mentor one or more graduate students beginning in the Fall of 2020 for at least one year. Mentoring students will be an important step forward for me as a professional scientist and future educator.

5. IMPORTANCE OF RESEARCH

Torch, and my research accompanying, will provide an unprecedented look into the star formation process, stellar feedback mechanisms, and young stellar cluster dynamics. By investigating star formation via detailed controlled experiments, I will be able to not only characterize the end-state of the star formation process but also identify any unique characteristics of massive star feedback effects during the transition phase between embedded and gas-free clusters. This work is vital to the field of star formation research as the process of ridding young clusters of their gas is not well understood nor entirely agreed upon. I am due to be the lead developer for Torch at Drexel, a framework that

offers a number of avenues of constant improvement, allowing for the sustained research of multiple graduate students and undergrads.

My research, although currently self-contained, has been developing along-side other graduate students and faculty in addition to my thesis advisors. Aaron Tran of Columbia University continues to help prime me for a more active development role for Torch. Graduate students Claude Cournoyer-Cloutier of McMaster University and Sabrina Appel of Rutgers University are currently developing branches of Torch; implementing stellar jets and primordial binary formation respectively. Will Farner of Drexel University has collaborated with me by analyzing output files from my runs detailed here, he also has begun work analyzing the consequences of our star placement algorithms and whether artificially inflated binary fractions are being created. Together, I hope to continue to our active collaboration and keep Torch a thriving source of new research opportunities.

The volume of data and insights received from my simulations will provide numerous starting points for other research projects, and I believe the collaborative efforts of the group will result in a number of publications that will give undergraduate students an opportunity to become involved and publish as co-authors.

Finally, this research is extraordinarily important to me as I believe it has the range, potential, and community interest necessary for the achievement of my professionally academic aspirations.

REFERENCES

- Baczynski, C., Glover, S. C. O., & Klessen, R. S. 2015, MNRAS, 454, 380
- Bonnell, I. A., Vine, S. G., & Bate, M. R. 2004, MNRAS, 349, 735
- Colin, P. et al., 2013, MNRAS, 435 ,2
- Dale, J. E., Ercolano, B., & Bonnell, I. A. 2012, MNRAS, 424, 377
- Dale, J. E., Ngoumou J., Ercolano B., Bonnell I. A., 2014, MNRAS, 442, 694
- Dobbs, C. L., Liow, K. Y., Rieder, S., 2020 MNRAS: Letters, 496, 1
- Domnguez, R., Fellhauer, M., Blaa, M. et al. J. 2017, MNRAS, 472, 465
- Draine, B. 2011a, Physics of the Interstellar and Intergalactic Medium, Princeton Series in Astrophysics (Princeton University Press)
- Federrath C., Banerjee R., Clark P. C., Klessen R. S., 2010, ApJ, 713, 269
- Fryxell B., et al., 2000, ApJS, 131, 273
- González-Samaniego, A. & Vazquez-Semadeni
- Jeans, J. H. (1902). "The Stability of a Spherical Nebula". Philosophical Transactions of the Royal Society A. 199: 1—53.
- Kroupa, P. 2001, MNRAS, 322, 231
- Krumholz M. R., et al., 2014, in Beuther H., Klessen R. S., Dullemond C. P., Henning T., eds, Protostars and Planets VI. p. 243 (arXiv:1401.2473),
- Lada, C. J., & Lada, E. A. 2003, Annual Review of Astronomy and Astrophysics, 41, 57
- Lanz, T., & Hubeny, I. 2003, ApJS, 146, 417
- MacNeice, P., Olson, K. M., Mobarry, C., de Fainchtein, R., & Packer, C. 2000, CoPhC, 126, 330
- McKee, C. F., & Ostriker, J. P. 1977, ApJ, 218, 148
- McKee, C. F. & Tan, J. C. 2003, ApJ, 585, 850
- McMillan, S., van Elteran, A., & Whitehead, A. 2012, in Astronomical Society of the Pacific Conference Series, Vol. 453, 129
- Olson, K. M., & MacNeice, P. 2005, in Adaptive Mesh Refinement—Theory and Applications, ed. T. Plewa, T. Linde, & V. G. Weirs (New York: Springer), 315
- Plunkett, A. L., Fernandez-Lpez, M., Arce, H. G. et al. 2018, A&A, 615, 9
- Portegies Zwart, S. F., & Verbunt, F. 1996, A&A, 309, 179
- Rahner D., Pellegrini E. W., Glover S. C. O., Klessen R. S., 2017, MNRAS, 470, 4453
- Stahler, S., & Palla, F. 2008, The Formation of Stars (Wiley)
- Truelove, J. K., Klein, R. I., McKee, C. F., et al. 1997, ApJ, 489, L179
- Turk M. J., Smith B. D., Oishi J. S., Skory S., Skillman S. W., Abel T., Norman M. L., 2011, ApJS, 192, 9
- Wall, J. E., McMillan, S. L. W., Low, M.-M. M., Klessen, R. S., & Zwart, S. P. 2019, The Astrophysical Journal, 887, 62
- Weaver, R., McCray, R., Castor, J., Shapiro, P., & Moore, R. 1977, ApJ, 218, 377
- Wolfire, M. G., McKee, C. F., Hollenbach, D., & Tielens, A. G. G. M. 2003, ApJ, 587, 278
- Zwart, S. P., McMillan, S. (2018). *Astrophysical Recipes The Art of AMUSE*. Institute of Physics Publishing